0090-9556/03/31001-76–87$7.00
DRUG METABOLISM AND DISPOSITION
Vol. 31, No. 01
801/1033593
Printed in U.S.A.

DMD 31:76–87, 2003

METABOLISM, PHARMACOKINETICS, AND EXCRETION OF A HIGHLY SELECTIVE *N*-METHYL-D-ASPARTATE RECEPTOR ANTAGONIST, TRAXOPRODIL, IN HUMAN CYTOCHROME P450 2D6 EXTENSIVE AND POOR METABOLIZERS

KIM JOHNSON, AJIT SHAH, SARAH JAW-TSAI, JAMES BAXTER, AND CHANDRA PRAKASH

Departments of Pharmacokinetics, Dynamics, and Metabolism (K.J., S.J., J.B., C.P.) and Clinical Sciences (A.S.), Pfizer Global Research and Development, Groton, Connecticut

(Received May 21, 2002; accepted September 28, 2002)

This article is available online at http://dmd.aspetjournals.org

ABSTRACT:

The excretion, biotransformation, and pharmacokinetics of a selective *N*-methyl-D-aspartate receptor antagonist, traxoprodil, were investigated in six healthy male volunteers, phenotyped either as CYP2D6 extensive or poor metabolizers of dextromethorphan. Each subject received an i.v. infusion of a single 50-mg (100 μCi) dose of [^{14}C]traxoprodil. Approximately 89% of the administered dose was recovered in poor metabolizers (PMs) and 61% in extensive metabolizers (EMs), with the majority of the dose being excreted in the urine (86% in PMs and 52% in EMs). The elimination of traxoprodil was more rapid in EMs than in PMs with terminal elimination half-lives of 2.8 and 26.9 h, respectively, for EMs and PMs. Area under the plasma concentration-time curve from time 0 to T ($AUC_{(0\text{-}Tlast)}$) values for unchanged traxoprodil were 1.2 and 32.7% of the corresponding AUC values for total radioactivity in EMs and PMs, respectively. Traxoprodil was metabolized in both EMs and PMs, with ~7 and 50% of the administered radioactivity excreted as unchanged drug in the excreta of EMs and PMs, respectively. Hydroxylation at the 3-position of the hydroxyphenyl ring and methylation of the resulting catechol followed by conjugation were identified as the main metabolic pathways in EMs. In contrast, direct conjugation of traxoprodil with glucuronic or sulfuric acid was the major pathway in PMs. In vitro studies using CYP2D6-selective inhibitor and recombinant enzyme also support that the metabolism of traxoprodil is mainly mediated by CYP2D6. Taken together, these studies suggest that traxoprodil is eliminated mainly by Phase I oxidative metabolism mediated by CYP2D6 isozyme in EMs and by Phase II conjugation and renal clearance of parent in PMs.

Traxoprodil[1] [CP-101,606; (1*S*,2*S*)-1-(4-hydroxyphenyl)-2-(4-hydroxy-4-phenylpiperidino)-1-propanol mesylate; Fig. 1] is a NMDA receptor antagonist currently undergoing clinical evaluation for the prevention of neuronal death associated with neurodegenerative diseases and brain injury (Chenard et al., 1995). It is highly selective for receptors containing NR2B subunits, which are expressed in forebrain neurons (Chenard et al., 1995; Menniti et al., 1997, 1998). In vitro, it inhibits the glutamate-induced death of rat hippocampal neurons (IC_{50} = 11 nM) and antagonizes NMDA-mediated responses in both hippocampal and cortical neurons (Chenard et al., 1995; Menniti et al., 1997). In vivo, it has been shown to be neuroprotective in two different animal models of traumatic brain injury and ischemia (Di et al., 1997; Tsuchida et al., 1997; Menniti et al., 2000). In addition, it has potent analgesic activity in rat hyperalgesia and nociceptive tests without affecting locomotor activity or causing the behavioral side effects often observed with currently available NMDA receptor antagonists (Taniguchi et al., 1997; Boyce et al., 1999). Phase I clinical trials in normal volunteers have shown that it is well tolerated at plasma concentrations two to three times the efficacious concentration in animal models of brain injury. Phase II studies in head trauma patients suggest that traxoprodil infused for up to 72 h is well tolerated, penetrates the cerebrospinal fluid and brain, and may improve outcome in brain-injured patients (Bullock et al., 1999; Merchant et al., 1999).

Metabolism and excretion studies of traxoprodil in rats and dogs after administration of a single i.v. dose have shown that it undergoes metabolism through oxidative pathways and conjugation, yielding metabolites that are eliminated primarily through bile in rats and via urine and bile in dogs (Prakash et al., 1997a). The main metabolic pathways in rats included aromatic oxidation at the phenyl ring attached to the piperidine, hydroxylation at the 3-position of the hydroxyphenyl ring, methylation of the resulting catechol intermedi-

[1] Abbreviations used are: Traxoprodil, CP-101,606, [(1*S*,2*S*)-1-(4-hydroxyphenyl)-2-(4-hydroxy-4-phenylpiperidino)-1-propanol mesylate]; NMDA, *N*-methyl-D-aspartate; EM, extensive metabolizer; PM, poor metabolizer; LC/MS/MS, liquid chromatography-tandem mass spectrometry; P450, cytochrome P450; HPLC, high performance liquid chromatography; LSC, liquid scintillation counting; Kel, the terminal phase rate constant; $T_{1/2}$, terminal phase half-life; $AUC_{0\text{-}T}$, area under the plasma concentration-time curve from time 0 to T; $AUMC_{0\text{-}T}$, area under the moment curve from time 0 to T; CL_p, systemic plasma clearance; MRT, mean residence time; VD_{ss}, steady-state volume of distribution; β-RAM, radioactive monitor; CAD, collisionally activated dissociation; amu, atomic mass unit(s); MS, mass spectrometry; 3-hydroxy-traxoprodil, 4-[1-hydroxy-2-(4-hydroxy-4-phenyl-piperidin-1-yl)-propyl]-benzene-1,2-diol; 3-methoxy-traxoprodil, 1-(4-hydroxy-3-methoxyphenyl)-2-(4-hydroxy-4-phenylpiperidino)-1-propanol; 4′-hydroxy-traxoprodil, 1-[2-hydroxy-2-(4-hydroxy-phenyl)-1-methylethyl]-4-(4-hydroxy-phenyl)-piperidin-4-ol; 2-OMe-E_2, 2-methoxy-17β-estradiol; 2-OH-E_2-3ME, 2-hydroxy-17β-estradiol-3-methyl ether.

Address correspondence to: Chandra Prakash, Ph.D., Pharmacokinetics, Dynamics, and Metabolism, Pfizer Global Research and Development, Groton, CT 06340. E-mail: Chandra_prakash@groton.pfizer.com

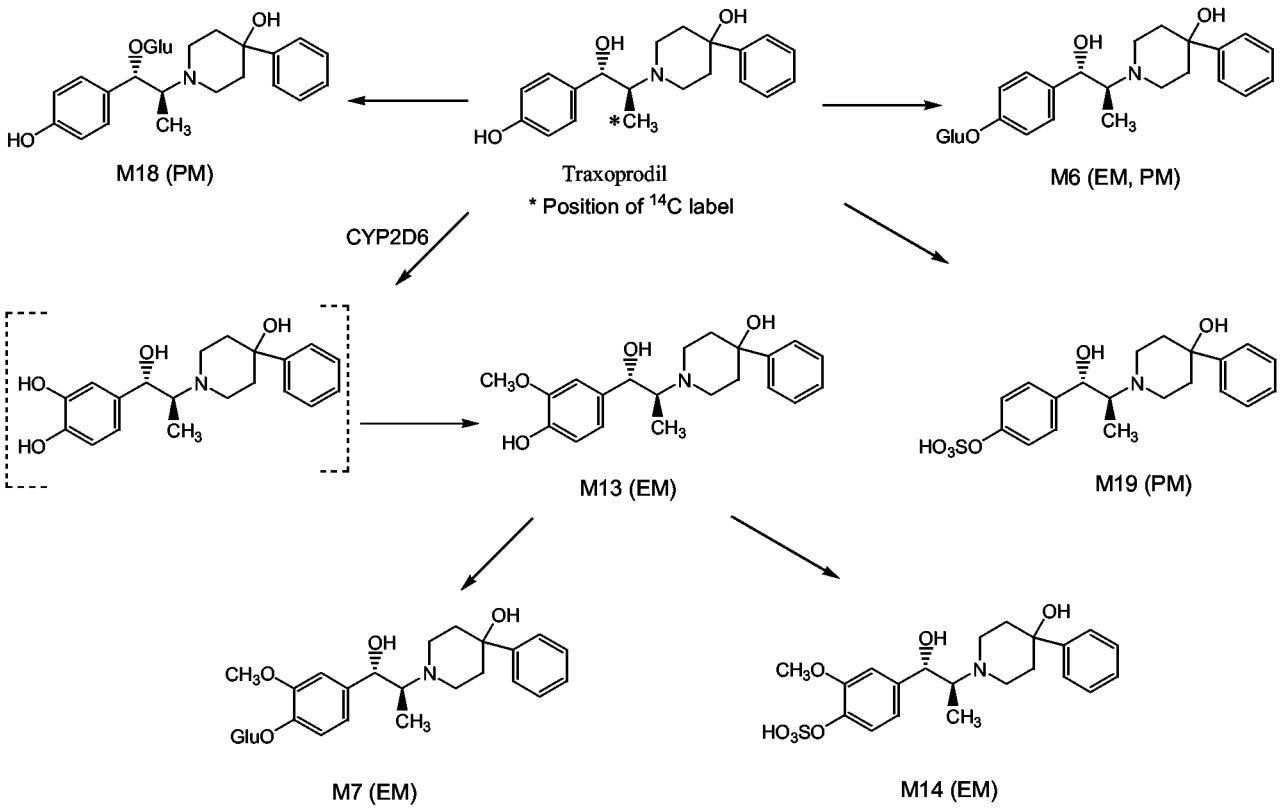

FIG. 1. *Biotransformation pathways for traxoprodil in humans.*

ates, and conjugation with glucuronic acid. Human pharmacokinetic studies following single i.v. and multiple oral dosing have shown considerable intersubject variability (A. Shah, unpublished work). This variability may be largely due to genetically determined metabolic pathways (Balant and Gex-Fabry, 1994).

The objectives of this study were to quantitatively determine the pharmacokinetics, metabolism, and excretion of traxoprodil and its metabolites in both EMs and PMs of dextromethorphan after an i.v. infusion of [^{14}C]traxoprodil (50 mg, ~100 μCi). Traxoprodil metabolism studies were also conducted with human liver microsomes and recombinant CYP2D6 microsomes in the presence and absence of quinidine, a specific inhibitor of CYP2D6. The metabolites were characterized by LC/MS/MS and, where possible, the proposed structures were supported by comparisons of their retention times on HPLC and MS spectra with those of synthetic standards.

Materials and Methods

General Chemicals. Commercially obtained chemicals and solvents were of HPLC or analytical grade. β-Glucuronidase (from *Helix pomatia*, type H-1 with sulfatase activity) was obtained from Sigma-Aldrich (St. Louis, MO). BDS hypersil C_{18} HPLC analytical and preparative columns were obtained from Thermo Hypersil, Keystone Scientific Operations (Bellefonte, PA). Ecolite (+) scintillation cocktail was obtained from ICN Biomedicals Inc. (Costa Mesa, CA). Carbosorb and Permafluor E^+ scintillation cocktails were purchased from PerkinElmer Life Sciences (Boston, MA). HPLC grade acetonitrile, methanol, and water were obtained from J. T. Baker (Phillipsburg, NJ). HPLC grade ammonium acetate and acetic acid were obtained from Fisher Scientific Co. (Fair Lawn, NJ). Diazomethane was generated just before use from 1-methyl-3-nitro-1-nitrosoguanidine obtained from Aldrich Chemical Co. (Milwaukee, WI).

Radiolabeled Drug and Reference Compounds. [^{14}C]Traxoprodil was synthesized by the Radiosynthesis Group at Pfizer Global Research and Development (Groton, CT) as described (McCarthy et al., 1997). [^{14}C]Traxoprodil showed a specific activity of 0.66 mCi/mmol and a radiochemical purity of >98%, as determined by HPLC using an in-line radioactivity detector. The dosing formulation was prepared as a sterile infusion and supplied as an open label supply. The synthetic standards, 3-hydroxy-, 3-methoxy-, and 3-hydroxy-4-*O*-methyltraxoprodil were synthesized by the Medicinal Chemistry Group at Pfizer Global Research and Development as described (Chenard et al., 1995).

Subjects and Dose Administration. Six normal healthy male subjects [four subjects phenotyped as CYP2D6 EMs and two subjects as PMs based on dextromethorphan to dextrorphan metabolic ratios] between the ages of 18 and 45 years participated in the study. Their metabolic ratios were defined as the ratio of the plasma concentrations of dextromethorphan to dextrorphan at 3 h after oral administration of dextromethorphan (Shah et al., 1998). The metabolic ratios for the EMs were 0.0040, 0.0023, 0.0022, and 0.0029, and for the PMs they were 1.32 and 0.893. The study protocol was reviewed and approved by the Institutional Review Board at the Clinical Research Facility of PPD Pharmaco (Austin, TX). After being informed of the purpose, design, and potential risks of the study, the volunteers gave written consent. Subjects entered the clinical testing facility approximately 12 h before dosing, and remained there for up to 216 h after dosing under continuous medical observation. All subjects fasted for at least 8 h prior to dosing and were given an i.v. infusion (2 h) of 50 mg dose of [^{14}C]traxoprodil (~100 μCi/subject). A standard meal was provided 4 h later. Subjects were required to refrain from lying down, eating, or drinking caffeinated and carbonated beverages during the first 4 h after drug administration.

Sample Collection. After dosing, urine samples were collected for up to 9 days at 0 to 12, 12 to 24, 24 to 48, 48 to 72, 72 to 96, 96 to 120, 120 to 144, 144 to 168, 168 to 192, and 192 to 216 h after the start of infusion. The total volumes of urine samples were recorded after each collection. Feces were collected as passed, from time of dosing until up to 216 h after the start of infusion.

Blood sufficient to provide a minimum of 6 ml of plasma was collected in heparinized tubes, from each subject at 0 (just before the start of infusion), 1, 2, 4, 8, 12, 16, 24, 36, 48, 72, 120, 144, 168, 192, and 216 h after the start of infusion. For metabolite identification blood sufficient to yield 20-ml plasma

was collected at 2, 6, and 24 h after the start of infusion. Within 1 h after collection, the blood samples were centrifuged in a refrigerated centrifuge, and plasma was separated from the whole blood. Samples (6 ml) collected over the first 216 h postdose were equally divided into two aliquots (3 ml each). One 3-ml aliquot from each sample collected over the first 216 h postdose was used for the quantitation of unchanged traxoprodil and its methoxy metabolite. The remaining 3-ml aliquots for the 0 to 216 h postdose samples were used for the quantitation of total radioactivity. All samples were labeled and immediately frozen and stored at −20°C until shipment for assays.

Determination of Radioactivity. Radioactivity in urine, feces, and plasma was measured by LSC. Aliquots of plasma and urine (0.3–1.0 ml, in triplicate) for each sampling time were mixed with 10 ml of scintillation fluid and counted in a liquid scintillation counter (Wallac 1409; PerkinElmer Wallac, Gaithersburg, MD). Fecal samples were placed into Stomacher 3500 bags and homogenized with equal amounts of water to thick slurry, using a Stomacher homogenizer (Cooke Laboratory Products, Alexandria, VA). Following the addition of CumbustAid (Packard, Downers Grove, IL), aliquots (~0.2 g, in triplicate) of the fecal homogenates were combusted in the oxidizer (Packard, model 307). Radioactivity in the combustion products was determined by trapping the liberated CO_2 in Carbo-sorb and Permafluor E^+ as scintillation cocktails, followed by liquid scintillation counting. Combustion efficiency was determined by combustion of the ^{14}C-labeled standards in an identical manner. Radioactivity less than twice the background value was considered to be below the limit of determination. The samples collected prior to dosing were used as controls and counted to obtain background count rate.

The radioactivity in the actual dose was expressed as 100%, and the radioactivity in urine and feces at each sampling time was defined as the percentage of dose excreted in the matrices at that sampling time. The amount of radioactivity in plasma was expressed as nanogram-equivalents of parent drug per milliliter and was calculated by using the specific activity of the dose administered.

Pharmacokinetic Analysis. Plasma concentrations of unchanged traxoprodil and its methoxy metabolite were determined at Phoenix Life Sciences (Saint-Laurent, Quebec Canada) by a validated HPLC/MS/MS assay. The assay exhibited a linear dynamic range of 2 to 500 ng/ml for traxoprodil and 3 to 500 ng/ml for 3-OMe-traxoprodil. The precision (relative standard deviation %) and accuracy (deviation %) values for the assay were within ±12.7 and ±3.9%, respectively. Pharmacokinetic parameters were determined using the Drug Metabolism Department "PK_PARAM" (version 1.039, 4/9/93) group procedure for RS/1 (Release 4.3.1; Bolt Beranek and Newman Inc., Cambridge, MA). Pharmacokinetic parameters were estimated using the following methods. Kel, the terminal phase rate constant, was estimated using the least-squares regression analysis of the plasma concentration-time data obtained during the apparent log-linear terminal phase. The terminal phase half-life ($T_{1/2}$) was calculated as 0.693/Kel. The maximal observed plasma concentration (C_{max}) and the time at which C_{max} was first observed (T_{max}) were determined by inspection of the data. The area under the plasma concentration-time curve from time 0 to T ($AUC_{0\text{-}T}$, where T is the time at which the last measurable drug concentration was observed) was calculated using the linear trapezoidal rule. The area from T to infinity was estimated as C_{est}/Kel, where C_{est} represents the estimated concentration at T based upon the aforementioned linear regression analysis. The total area under the curve was estimated as the sum of the two [i.e., $AUC_{0\text{-}\infty} = (AUC_{0\text{-}T} + AUC_{T\text{-}\infty})$]. The area under the moment curve from time 0 to T ($AUMC_{0\text{-}T}$) was calculated by the linear trapezoidal rule. $AUMC_{T\text{-}\infty}$ was estimated as $(T \cdot C_{est}/Kel)+(C_{est}/Kel^2)$, and $AUMC_{0\text{-}\infty}$ was the sum of the two [i.e., $AUMC_{0\text{-}\infty} = (AUMC_{0\text{-}T} + AUMC_{T\text{-}\infty})$]. Systemic plasma clearance (CL_p) was determined as Dose/$AUC_{0\text{-}\infty}$. Mean residence time (MRT) was determined as $(AUMC_{0\text{-}\infty}/AUC_{0\text{-}\infty})-(\tau/2)$, in which τ = total duration of the iv infusion. Steady-state volume of distribution (VD_{ss}) was calculated as $CL_p \cdot MRT$.

Plasma concentrations below the lower limit of quantitation were treated as 0.0 ng/ml for purposes of calculating mean and standard deviation (S.D.) of plasma concentrations at each sampling time and for calculating pharmacokinetic parameters. Standard deviations were determined for a time point when at least 50% of values had measurable plasma concentrations.

Extraction of Metabolites from Biological Samples. Aliquots (~50 ml) of urine samples collected from EMs at 0 to 12, 12 to 24, and 24 to 48 h and from PMs at 0 to 12, 12 to 24, 24 to 48, and 48 to 72 h after the start of infusion were pooled on the basis of volume collected at respective time intervals. The pooled urine samples (~10 ml) were passed over a preconditioned C_{18} solid phase extraction column (Supelco, Bellefonte, PA). The column was washed with water (10 ml), and the radioactivity was eluted with 10 ml of methanol. The methanolic eluate was concentrated under nitrogen. The residues were reconstituted in 0.3 ml of methanol/10 mM ammonium acetate (1:1), and aliquots (100 μl) were injected into the HPLC system.

Aliquots of the fecal homogenates from both EMs and PMs at 0 to 144 h postdose were pooled, and the pooled fecal samples (100–200 g) were diluted with methanol (400–600 ml). The suspensions were stirred for 2 h on a magnetic stirrer, sonicated for 10 min, and centrifuged. The supernatants were separated and the residues further extracted with 5 × 100 ml of methanol. The supernatants were combined and 1-ml aliquots were counted in a liquid scintillation counter. The organic extracts were evaporated to dryness on a rotary evaporator, and the residues were reconstituted in methanol/water (1:1). Aliquots (1 ml) of concentrated fecal extracts were injected into the preparative HPLC column. Fractions were collected at 0.5-min intervals, mixed with scintillation cocktail, and quantitated by LSC. The pellets remaining after extraction were dried, combusted, and also quantitated by LSC.

Plasma samples (1–20 ml) from each subject at 2, 6, and 24 h after the start of infusion were mixed with 5 volumes of acetonitrile, vortexed, and sonicated. The mixtures were centrifuged and the supernatants removed. This procedure was repeated several times until no radioactivity was observed in the supernatant. Aliquots of each extract were quantitated by LSC, and the remaining supernatants were combined and concentrated to dryness under nitrogen. The residues were reconstituted in 1500 μl of water, centrifuged to remove insoluble matters, and 1000-μl aliquots were injected into the preparative HPLC column. Fractions were collected at 0.5-min intervals, mixed with scintillation cocktail, and quantitated by LSC.

Derivatization. Urine samples were methylated with diazomethane as previously described (Prakash et al., 1997b). Aliquots (100 μl) of the concentrated urine samples were dissolved in methanol (100 μl), and freshly prepared ethereal diazomethane (200 μl) was added. After standing for 30 min at room temperature, the solvent was removed by a stream of nitrogen, and the residue was dissolved in the HPLC mobile phase.

Enzymatic Hydrolysis. The concentrated urine samples (0.5 ml) were adjusted to pH 5 with sodium acetate buffer (0.1 M) and treated with 2,500 units of β-glucuronidase/sulfatase (Prakash and Soliman, 1997). The mixture was incubated in a shaking water bath at 37°C for 12 h and was diluted with acetonitrile. The precipitated protein was removed by centrifugation. The pellet was washed with an additional 2 ml of acetonitrile, and the two supernatants were combined. The supernatant was concentrated and dissolved in 0.5 ml of mobile phase, and an aliquot (50 μl) was injected into the HPLC system. Incubation of urine samples for 12 h without the enzyme served as a control.

Microsome Incubations and Inhibition Studies. Human liver samples were obtained from organ donors and stored at −70°C until used. Human microsomes were obtained by homogenization of liver sample in 0.25 M potassium phosphate buffer (pH 7.25) containing 1 mM EDTA and 0.15 M KCl, followed by differential centrifugation using published procedures (Prakash et al., 2000). Protein concentrations were measured by the bincinchoninic acid assay, using bovine serum albumin as the standard, and the P450 concentrations were determined by the method of Omura and Sato (1964). The microsomes from a single human liver (age 58, white male) preparation were used in this study. The microsomal preparation was characterized for the following five major drug metabolizing P450 isoforms: CYP1A2, CYP2C9, CYP2C19, CY2D6, and CYP3A4. The enzymatic activities of P450 isoforms in microsomes were determined by phenacetin *O*-deethylase for CYP1A2 (Tassaneeyakul et al., 1993), tolbutamide hydroxylase for CYP2C9 (Miners et al., 1988), (*S*)-mephenytoin hydroxylase for CYP2C19 (Meier et al., 1985), bufuralol 1′-hydroxylase for CYP2D6 (Kronbach et al., 1987), and testosterone 6β-hydroxylase for CYP3A4 (Sonderfan et al., 1987) and were 0.315, 0.22, 0.055, 0.088, and 2.2 nmol/min/mg of microsomal protein, respectively. Recombinant CYP2D6 was expressed in insect cells, and microsomal subcellular fractions were prepared by standard centrifugation procedures. The activity of expressed CYP2D6 (bufuralol 1′-hydroxylation) was 0.91 nmol/min/mg of microsomal protein. The microsomal fractions were stored at −70°C until used.

TABLE 1

Percentage of radioactivity excreted after a single 50 mg 2 h i.v. infusion of [^{14}C]traxoprodil in male subjects

Time Interval	EM[a]			PM[b]		
	Urine	Feces	Total	Urine	Feces	Total
h						
0–12	38.4 ± 3.59	ns	38.4 ± 3.59	22.6, 22.7	ns, ns	22.6, 22.7
0–24	7.83 ± 2.58	0.1 ± 0.0	7.93 ± 2.54	17.4, 19.5	0.10, 0.13	17.5, 19.6
24–48	3.87 ± 0.74	0.92 ± 1.66	4.79 ± 1.72	17.4, 20.3	0.59, 2.09	18.0, 22.4
48–72	0.89 ± 0.24	5.33 ± 2.50	6.22 ± 2.55	10.8, 11.0	0.69, 0.00	11.5, 11.0
72–96	0.28 ± 0.09	1.8 ± 1.23	2.08 ± 1.29	6.00, 5.54	0.69, 1.29	6.69, 6.83
96–120	0.22 ± 0.12	0.14 ± 0.1	0.36 ± 0.24	6.46, 3.16	ns, ns	6.46, 3.16
120–216	0.25 ± 0.07	0.67 ± 0.37	0.92 ± 0.41	4.39, 4.20	0.82, 0.62	5.21, 4.82
Total	51.7 ± 3.6	8.96 ± 2.46	60.7 ± 1.6	85.0, 86.4	2.89, 4.13	87.9, 90.5

ns, no sample.
[a] $N = 4$ (mean ± S.D.).
[b] $N = 2$ (individual values).

The microsomal incubation mixtures contained a 2 mg/ml microsomal protein, an NADPH generating system (0.5 mM $NADP^+$, 4 mM glucose 6-phosphate, and 10 U/ml glucose-6-phosphate dehydrogenase), 0.1 M phosphate buffer (pH 7.4), 10 mM $MgCl_2$, and traxoprodil (0–100 μM) in a total volume of 1 to 2.5 ml. The reaction mixtures were preincubated at 37°C for 2 min prior to initiation of the reaction by the addition of traxoprodil. The incubations were conducted in a 37°C water bath with gentle shaking. The reaction was stopped by the addition of an equal volume of cold acetonitrile. The denatured protein was separated by centrifugation, and the resulting supernatant was transferred and evaporated in a nitrogen evaporator. Samples were dissolved in HPLC mobile phase (83% 50 mM KH_2PO_4, 15% CH_3OH, 2% tetrahydrofuran, and 0.1% tetraethylammonium) and then analyzed by HPLC as described herein. Controls were incubated either without NADPH or without microsomes. Incubation conditions were chosen to ensure linear production of metabolite to determine the kinetic parameters of the reaction precisely. Apparent K_m and V_{max} values for the formation of hydroxy metabolite were estimated from the Michaelis-Menten equation using nonlinear curve fitting (Sigma plot; SPSS Sciences, Chicago, IL). Inhibition studies were performed using a pool of human liver microsomes and a specific CYP2D6 inhibitor, quinidine (0.1, 1, 10, and 100 μM).

HPLC. The analytical HPLC system consisted of a HP-1100 solvent delivery system, a HP-1100 membrane degasser, an HP-1100 autoinjector (Hewlett Packard, Palo Alto, CA), a Thermo Separations spectromonitor 3200 UV (San Jose, CA), and a radioactive monitor (β-RAM; IN/US, Tampa, FL). Chromatography was performed on a BDS hypersil C_{18} column (4.6 mm x 250 mm, 5 μm) with a mobile phase containing a mixture of 10 mM ammonium acetate (solvent A) and acetonitrile (solvent B). The mobile phase was initially composed of solvent A/solvent B (95:5), and held for 10 min. The mobile phase composition was then linearly programmed to solvent A/solvent B (75:25) over 20 min and held at these conditions for 2 min. A short gradient to solvent A/solvent B (10:90) over 3 min was used to flush the column. The mobile phase composition was returned to the starting solvent mixture over 3 min. The system was allowed to equilibrate for approximately 15 min before making the next injection. A flow rate of 1.0 ml/min was used for all analyses.

The preparative HPLC system consisted of a Gilson 322 solvent delivery system, membrane degasser, a Gilson 215 autoinjector (Middletown, WI), a Thermo Separations spectromonitor 3200 UV and a β-RAM (IN/US). Chromatography was performed on a BDS hypersil C_{18} column (10 mm × 250 mm, 5 μm) with a mobile phase containing a mixture of 10 mM ammonium acetate (solvent A) and acetonitrile (solvent B). The mobile phase was initially composed of solvent A/solvent B (95:5) and held for 5 min. The mobile phase composition was then linearly programmed to solvent A/solvent B (75:25) over 30 min and held at these conditions for 1 min. A short gradient to solvent A/solvent B (20:80) over 3 min was used to flush the column. The mobile phase composition was returned to the starting solvent mixture over 3 min. The system was allowed to equilibrate for approximately 15 min before making the next injection. A flow rate of 4.0 ml/min was used for all analyses.

From microsomal incubations, traxoprodil and its hydroxy metabolite were quantitated by HPLC with UV detection at 226 nm. The metabolites were separated on a Zorbax SB-CN HPLC column (2.1 mm x 150 mm, 3 μm) with a mobile phase consisting of 50 mM potassium phosphate/methanol/tetrahydrofuran/tetraethylammonium (85:12:3:0.1) at a flow rate of 0.25 ml/min.

Quantitative Assessment of Metabolite Excretion. Quantification of the metabolites was carried out by measuring radioactivity in the individual HPLC-separated peaks using a β-RAM. The β-RAM provided an integrated printout in counts per minute and percentage of the radiolabeled material, as well as peak representation. The β-RAM was operated in the homogeneous liquid scintillation counting mode, with addition of 3 ml/min of Tru-Count (+) scintillation cocktail to the effluent after UV detection. The radiochromatograms of metabolites in plasma and feces were generated by collecting fractions at 30-s intervals and counting the fractions in a Wallac 1409 liquid scintillation counter. The retention times of the radioactive peaks, where possible, were compared with those of synthetic standards and/or metabolites obtained from the rat urine.

LC/MS/MS. LC/MS/MS was conducted with a Finnigan TSQ 7000 (Thermo Finnigan MAT, San Jose, CA) equipped with an electrospray ion source. The effluent from the HPLC column was split, and about 50 μl/min was introduced into the atmospheric ionization source. The remaining effluent was directed into the flow cell of the β-RAM. The β-RAM response was recorded in real time by the mass spectrometer data system, which provided simultaneous detection of radioactivity and MS data. The electrospray interface was operated at 4500 V, and the mass spectrometer was operated in the positive ion mode. CAD studies were performed using argon gas at collision energy of 20 to 40 eV and at a pressure of 2 mTorr. Data were processed with a computer operating ICIS 3.2.1 and Xcalibur (Thermo Finnigan MAT).

Results

Mass Balance. As shown in Table 1, after iv infusion of 50-mg dose of [^{14}C]traxoprodil to human subjects, the administered radioactivity was eliminated predominantly in the urine. At 216 h after the start of infusion, the mean cumulative urinary excretion amounted to 51.7 and 85.7% for EMs and PMs, respectively. The mean fecal recoveries were only 8.96% for EMs, and 3.61% for PMs. In total, 60.7 and 89.3% of the administered radioactive dose was recovered in urine and feces of EMs and PMs, respectively. Of the entire radioactivity recovered in urine of EMs, approximately 96.9% was excreted in the first 48 h. In contrast, the elimination of the administered radioactivity in the urine of PMs was slower. The radioactivity in the urine of PMs was excreted up to 168 h after the start of infusion. Because feces were collected after natural defecation, the fecal elimination of radioactivity was delayed in both EMs and PMs, compared with that in urine. The major portion of radioactivity in feces appeared during the 0- to 216-h time period after the start of infusion.

Pharmacokinetics. *Traxoprodil.* Mean plasma concentration-time curves for traxoprodil in EMs and PMs are shown in Fig. 2. Calculated pharmacokinetic parameters for the unchanged drug are presented in Table 2. Plasma concentrations for traxoprodil were in-

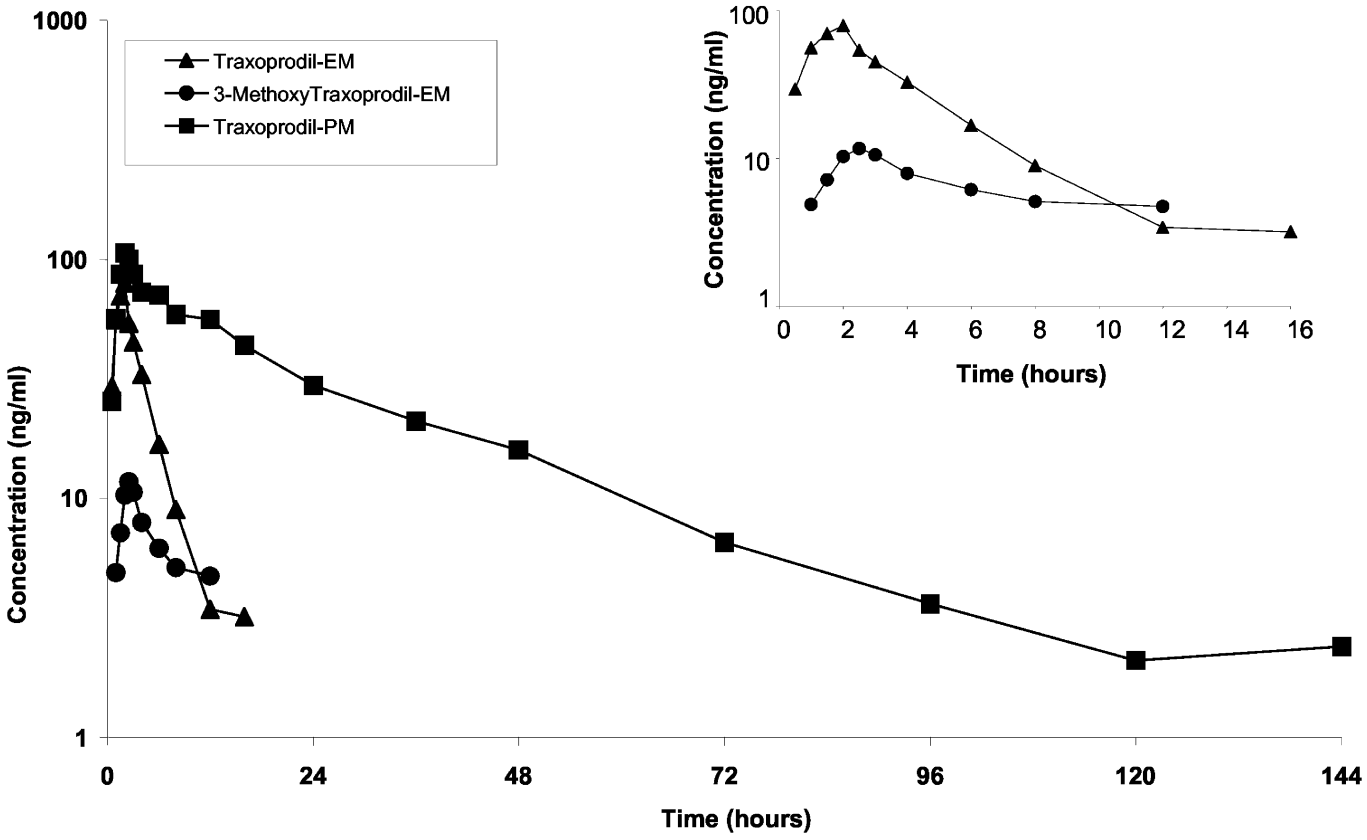

FIG. 2. *Mean plasma concentration-time curves of traxoprodil and 3-methoxy traxoprodil (EM) in human volunteers [PM (n = 2) and EM (n = 4)] after a single i.v. infusion of 50 mg of [^{14}C]traxoprodil.*

creased during the 2-h infusion period such that C_{max} was observed at the end of infusion (~2 h) for both EMs and PMs. On average, C_{max} was slightly higher in PM subjects, compared with EMs, with respective mean values of 105 and 79.2 ng/ml. A greater difference in overall systemic exposure was observed between PMs and EMs based on an $AUC_{0-\infty}$ comparison. Mean $AUC_{0-\infty}$ was approximately 8-fold greater in PMs, compared with EMs, with respective values of 2610 and 310 ng · h/ml. The mean CL_p was 2800 ml/min, mean VD_{ss} was 515 liters, and mean MRT was 3.1 h for EMs. For PMs, the mean CL_p was 323 ml/min, mean VD_{ss} was 637 liters, and mean MRT was 33.2 h. As expected, terminal phase half-lives were, on average, approximately 10-fold longer in PMs, with PM and EM values of 26.9 and 2.8 h, respectively.

Total Radioactivity. Mean plasma concentration-time curves of total radioactivity in EMs and PMs are shown in Fig. 3. Calculated pharmacokinetic parameters for the total radioactivity are presented in Table 2. Relative to parent drug, concentrations of total radioactivity peaked slightly later in both EMs and PMs with mean values of 3.8 and 5.0 h, respectively, after the start of infusion of the radiolabeled drug. C_{max} values for the total radioactivity ranged from 338 to 491 ng-Eq/ml with a mean value of 387 ng-Eq/ml for EMs, and from 146 to 171 ng-Eq/ml with a mean value of 159 ng-Eq/ml for PMs. Mean

TABLE 2

Pharmacokinetic parameters of traxoprodil, 3-methoxytraxoprodil and total radioactivity in humans following 2 h i.v. infusion of a single 50-mg dose of [^{14}C]traxoprodil

Analyte	CYP2D6 Phenotype[a]	$AUC_{(0-Tlast)}$[b]	$AUC_{0-\infty}$[b]	C_{max}[b]	T_{max}	$T_{1/2}$[c]	MRT	CL	VD_{ss}
		ng · h/ml	*ng · h/ml*	*ng/ml*	*h*	*h*	*h*	*ml/min*	*liter*
Traxoprodil	EM	299 ± 63	310 ± 66	79.2 ± 18.4	2.0 ± 0.0	2.8 ± 0.7	3.1 ± 0.4	2800 ± 669	515 ± 111
	PM	2790, 2270	2880, 2340	104, 106	3.0, 2.0	29.3, 24.5	36.2, 30.3	289, 356	628, 647
	Mean PM	2530	2610	105	2.5	26.9	33.2	323	637
3-Methoxy-traxoprodil	EM	57.2 ± 25.6	NC	11.7 ± 3.5	2.4 ± 0.3				
	PM								
Radioactivity	EM	25100 ± 3301	NC	387 ± 70	3.8 ± 0.5	146 ± 21			
	PM	8570, 6920	9230, 7430	171, 146	6.0, 4.0	46.0, 46.5			
	Mean PM	7745	8330	159	5.0	46.3			

NC, not calulated.
[a] EM (N = 4, mean ± S.D.); PM (N = 2, individual values).
[b] C_{max} and AUC values for total radioactivity are expressed as ng-Eq/ml and ng-Eq · h/ml, respectively.
[c] $T_{1/2}$ for the radioactivity was estimated as 146 h, therefore, $AUC_{(0-\infty)}$ values for total radioactivity were not calculated.

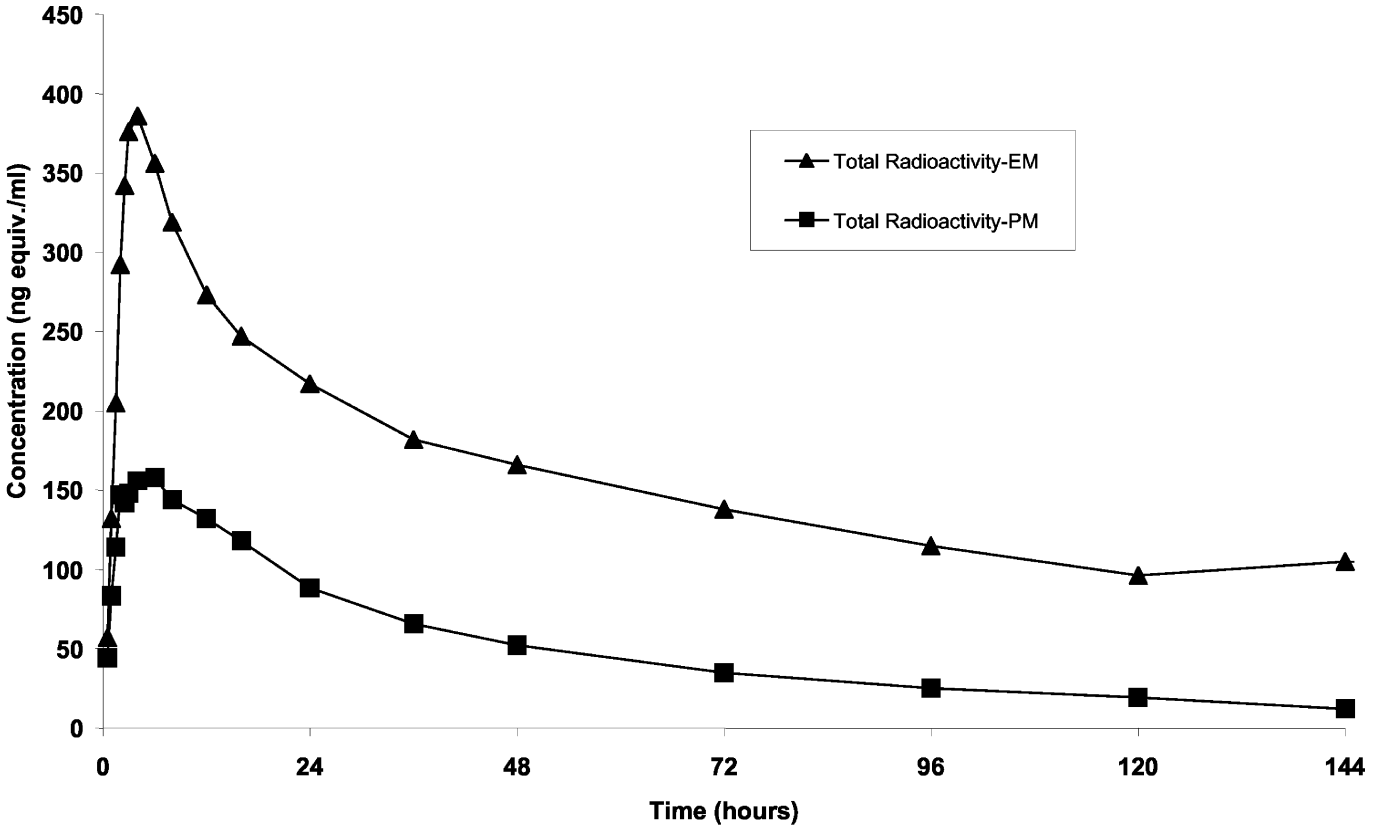

FIG. 3. *Mean plasma concentration-time curves of total radioactivity in human volunteers [PM (n = 2) and EM (n = 4)] after a single i.v. infusion of 50 mg of [^{14}C]traxoprodil.*

$AUC_{(0\text{-}Tlast)}$ values for total radioactivity were 25,100 and 7,745 ng-Eq · h/ml for EMs and PMs, respectively. The mean $T_{1/2}$ values were estimated as 146 h for EMs and 46.3 h for PMs. $AUC_{0\text{-}\infty}$ values for total radioactivity for EMs, however, could not be calculated due to the long estimated $T_{1/2}$.

3-Methoxymetabolite M13. Mean plasma concentration-time curve for M13 in EMs is shown in Fig. 2. The pharmacokinetic parameters for M13 are presented in Table 2. C_{max} values for the M13 metabolite ranged from 8.37 to 16.4 ng/ml with a mean value of 11.7 ng/ml in EMs. Mean $AUC_{(0\text{-}Tlast)}$ was 57.2 ng · h/ml. M13 was not detected in PMs.

Metabolic Profiles in Biological Samples. *Urine.* The representative HPLC radiochromatograms recorded with an in-line radioactivity detector, for urine from two human subjects (one PM and one EM) are shown in Fig. 4. In addition to unchanged drug, four metabolites in EMs and three metabolites in PMs were detected in the radiochromatograms. The percentages of metabolites excreted in urine are presented in Table 3 for both EMs and PMs. There were major phenotype related differences in the metabolism of traxoprodil in humans. In EMs, the major urinary metabolites were due to oxidation on the hydroxylphenyl ring followed by conjugation of the resulting catechol. In contrast, the urinary metabolites in PMs were due to direct conjugation with glucuronic acid or sulfuric acid. Unchanged traxoprodil (6.03%) and four metabolites, M6 (0.68%), M7 (8.83%), M13 (1.89%), and M14 (34.2%), were identified in the urine of EMs. The urinary metabolites in PMs were unchanged drug (48.4%), M6 (24.6%), M18 (1.4%), and M19 (11.3%).

Feces. The representative HPLC radiochromatograms for fecal metabolites from EMs and PMs are shown in Fig. 5. In addition to unchanged drug, one metabolite M19 (0.42%) in PMs, and two metabolites, M13 (1.1%) and M14 (4.26%), in EMs were identified. The percentages of fecal metabolites are presented in Table 3.

Circulating Metabolites. Approximately, 96, 95, and 88% of the radioactivity was recovered from the plasma of PMs at 2, 6, and 24 h, respectively, after extraction. In contrast, the recovery of the radioactivity from the plasma of EMs was 87, 61, and 25% at 2, 6, and 24 h, respectively. The representative HPLC radiochromatograms of circulating metabolites at 6 h samples of EMs and PMs are shown in Fig. 6. Traxoprodil and four metabolites (M6, M7, M13, and M14) in EMs and three metabolites (M6, M18, and M19) in PMs were detected in the radiochromatograms. The metabolites were similar to those found in urine. The relative percentage of circulating metabolites is presented in Table 4.

Identification of Metabolites *Metabolites M6 and M18.* M6 was detected both in EMs and PMs whereas M18 was detected only in PMs. The full-scan mass spectra of both M6 and M18 revealed a protonated molecular ion $[(M + H)^+]$ at *m/z* 504, 176 amu higher than the parent drug, indicating that these metabolites were the glucuronide conjugates. The CAD product ion spectra of *m/z* 504 of both M6 and M18 showed fragment ions at *m/z* 486 $(MH\text{-}H_2O)^+$, 328 (MH-glucuronide)$^+$, 310 (MH-glucuronide-H_2O)$^+$, 292 (MH-glucuronide-H_2O-H_2O)$^+$, 160 and 151. The prominent and significant ions at *m/z* 160 $[C_5H_{10}N(OH)C_6H_5\text{-}H_2O]^+$ and 151 $[C_6H_4(OH)CHOHCH_2CH_2^+]$ were similar to those of the parent drug, suggesting that both the phenylpiperidinol and the phenylethyl portions of the molecule were intact (Prakash et al., 1997a). Based on these data, M6 and M18 were identified as positional isomers with respect to the binding site of glucuronic acid. The site of glucuronidation was established by the electrospray ionization-MS and MS/MS analysis of the methylated products of these glucuronides.

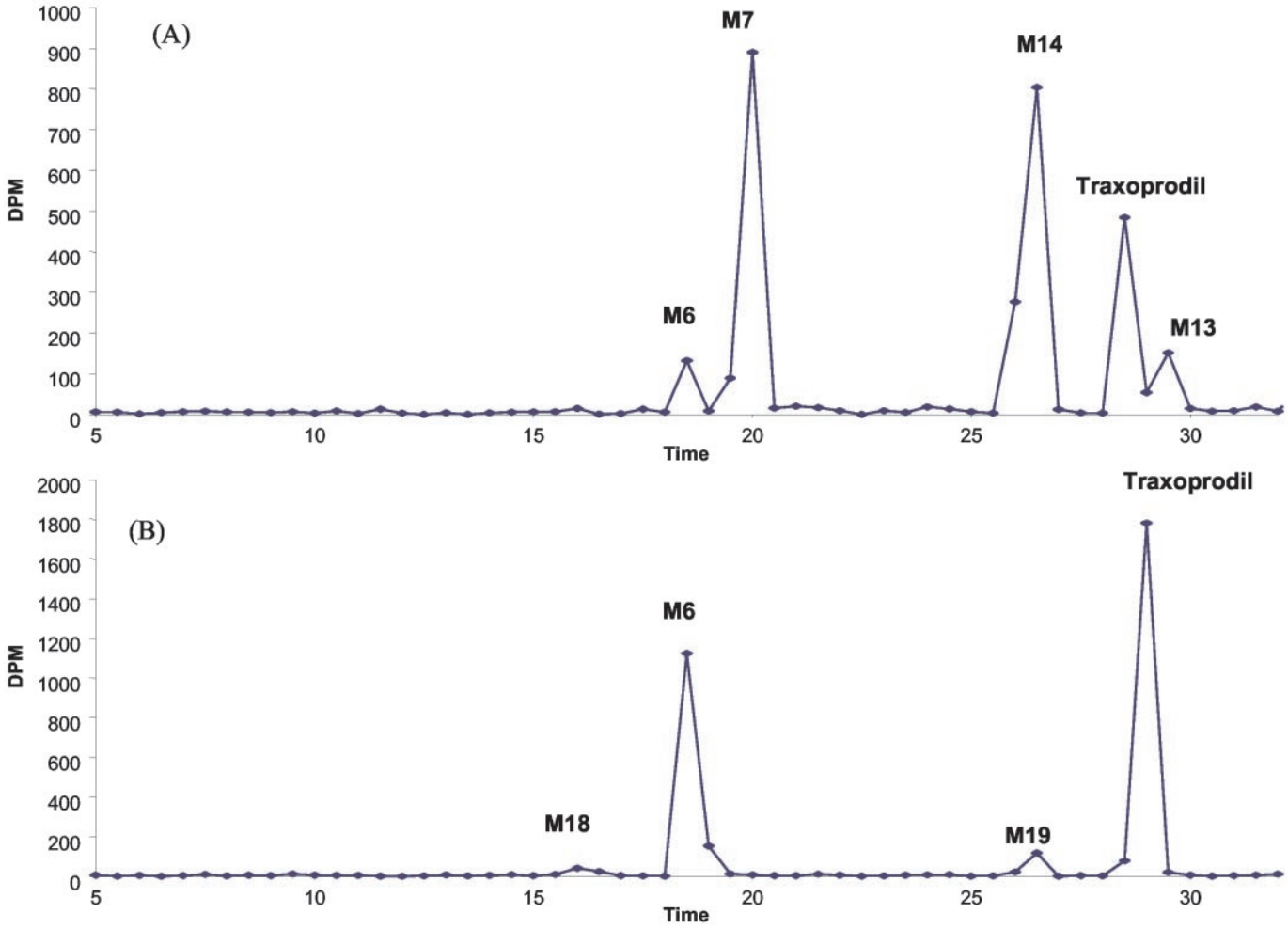

FIG. 4. *HPLC-radiochromatograms of traxoprodil metabolites in human urine of (A) EM and (B) PM after a single i.v. infusion of 50 mg of [^{14}C]traxoprodil.*

TABLE 3

Percentage of metabolites of traxoprodil in urine and feces of humans following 2 h i.v. infusion of a single 50-mg dose of [^{14}C]traxoprodil

Metabolite	Retention Time	% of Administered Dose					
		EM[a]			PM[b]		
		Urine	Feces	Total	Urine	Feces	Total
	min/s						
M18	17:47	nd	nd	nd	1.63, 1.17	nd	163, 1.17
M6	19:53	0.68 ± 0.04	nd	0.68 ± 0.04	25.2, 23.9	nd	25.2, 23.9
M7	21:04	8.83 ± 0.78	nd	8.83 ± 0.78	nd	nd	nd
M19	25:41	nd	nd	nd	11.2, 11.3	0.15, 0.68	11.4, 12.0
M14	26:00	34.2 ± 2.69	4.26 ± 0.82	38.5 ± 2.96	nd	nd	nd
Traxoprodil	28:33	6.03 ± 1.45	1.11 ± 0.60	7.14 ± 1.39	46.9, 49.9	2.03, 1.88	48.9, 51.8
M13	29:44	1.89 ± 0.08	1.11 ± 0.37	2.80 ± 0.69	nd	nd	nd

nd, not detected.
[a] EM (N = 4, mean ± S.D.).
[b] PM (N = 2, individual values).

After treatment of M6 with diazomethane, full-scan MS of the product showed an intense protonated molecular ion at *m/z* 518, 14 amu higher than M6, indicating the addition of one methyl group. The MS/MS spectrum of the ion *m/z* 518 showed fragment ions at *m/z* 500 $(MH\text{-}H_2O)^+$, 310, 292, 174, 160, and 151, similar to those obtained for parent drug (Fig. 7A). These results indicated that M6 was a phenolic glucuronide. On the other hand, the full scan MS of the methylated product of M18 showed an intense protonated molecular ion at *m/z* 532, 28 amu higher than M18, indicating the addition of two methyl groups. The MS/MS spectrum of *m/z* 532 showed fragment ions at *m/z* 514, 324, 306, 188, 176, and 160 (Fig. 7B). The ions at *m/z* 324, 306, and 188 were 14 amu higher than those obtained for the metabolite M18 and the parent drug. These data suggest that the phenolic group was unsubstituted for M18 and thus, M18 was identified as a benzylic glucuronide.

Metabolite M7. M7 was present only in urine and plasma of EMs. Full-scan mass spectrum of M7 revealed a protonated molecular ion at *m/z* 534, 206 amu higher than the parent drug, suggesting that it was

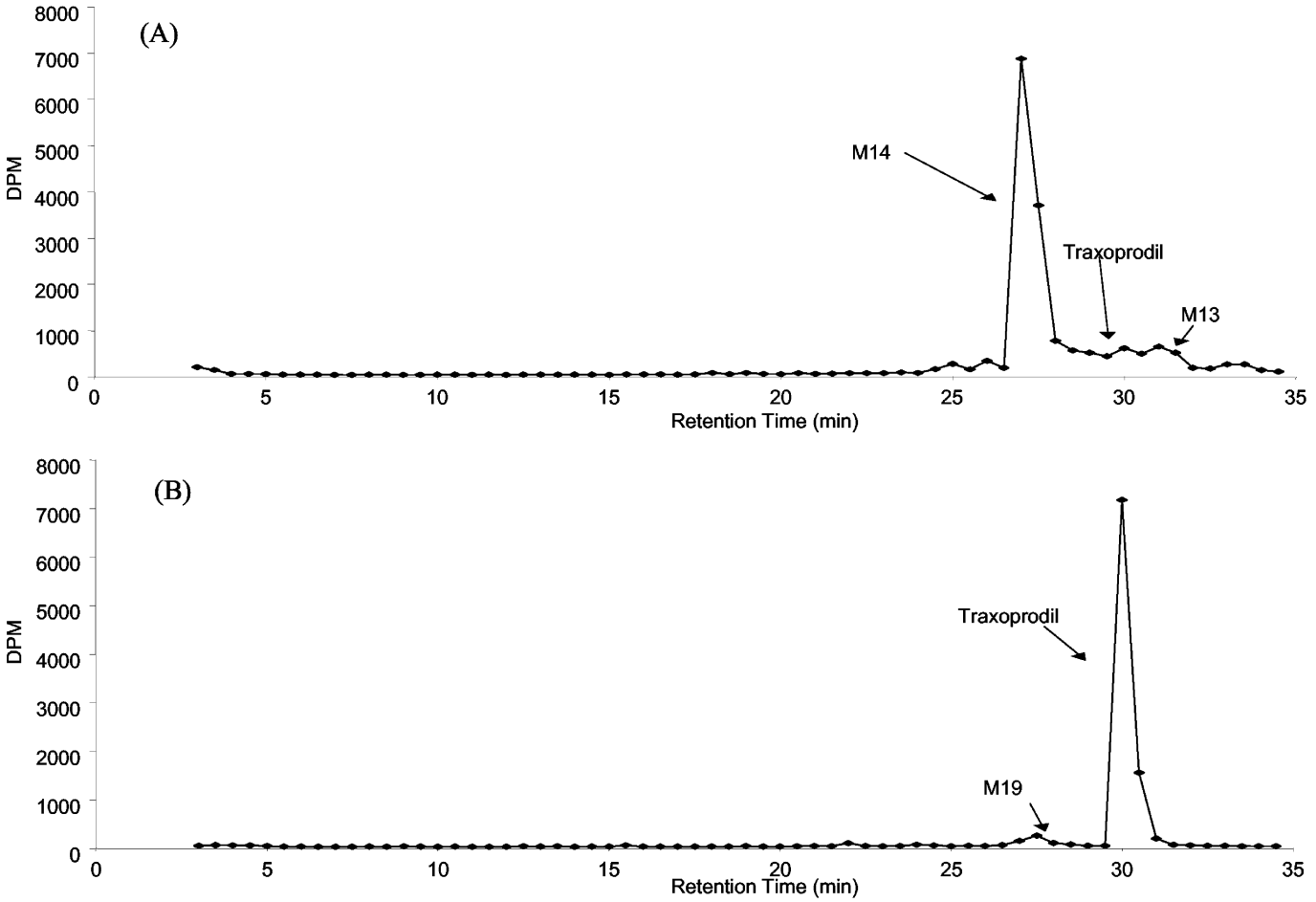

FIG. 5. *HPLC-radiochromatograms of traxoprodil metabolites in human feces of (A) EM and (B) PM after a single i.v. infusion of 50 mg of [^{14}C]traxoprodil.*

a conjugate. The MS/MS spectrum of the ion at *m/z* 534 gave the intense ions at *m/z* 516, 358, 340, 322, 181, and 160. The fragment ion at *m/z* 340, loss of 194 (176 + 18) amu from the precursor ion, suggested that it was a glucuronide conjugate. The fragment ion at *m/z* 181, 30 amu higher than that of the parent drug, suggested the addition of a methoxy group on the hydroxyphenyl ring. It was hydrolyzed to M13 on treatment with β-glucuronidase. Based on these data, M7 was identified as a glucuronide conjugate of M13.

Metabolite M13. M13 was present in urine, feces, and plasma of EMs. Full-scan mass spectrum of M13 revealed a protonated molecular ion at *m/z* 358, 30 amu higher than the parent drug, indicating that a methoxy group had been added to the molecule. The CAD product ion spectrum of the ion at *m/z* 358 gave intense ions at *m/z* 340, 322, 181, 160, 151, and 131. The fragment ions at *m/z* 160 and 131 suggested that the phenylpiperidinol moiety was unchanged. The ion at *m/z* 181 indicated that the methoxy group had been added to the phenyl-ethyl portion of the molecule. Its retention time on HPLC was similar to that of synthetic 3-methoxytraxoprodil. Based on these data, M13 was identified as 3-methoxytraxoprodil.

Metabolite M14. M14 was found only in EMs. Full-scan mass spectrum of M14 revealed a protonated molecular ion at *m/z* 438, 110 amu higher than the parent drug, suggesting that it was a conjugate. The CAD product ion spectrum of ion at *m/z* 438 gave intense fragment ions at *m/z* 340, 322, 181, and 160. The fragment ion at *m/z* 340, loss of 98 amu (80 + 18), suggested that M14 was a sulfate conjugate. The fragment ions at *m/z* 181 and 151 indicated that a methoxy group had been added to the hydroxyphenyl ring of the molecule. It was hydrolyzed to M13 on treatment with sulfatase. Thus, M14 was identified as a sulfate conjugate of M13.

Metabolite M19. M19 was found only in PMs. It showed a protonated molecular ion at *m/z* 408, 80 amu higher than the parent drug, suggesting that it was a sulfate conjugate. The CAD product ion spectrum of the ion at *m/z* 408 gave intense fragment ions at *m/z*, 310, 292, 188, 174, 160, 151, 133, and 121. The fragment ion at *m/z* 310, loss of 98 amu (80 + 18), suggested that M19 was a sulfate conjugate. It was hydrolyzed to traxoprodil on treatment with sulfatase. Thus, M19 was identified as a sulfate conjugate of traxoprodil.

Identification of the Major P450 Isoform Involved in Traxoprodil Metabolism. The major oxidative metabolite observed in human liver microsomal incubations was identified as the 3-hydroxytraxoprodil, which accounted for 84% of traxoprodil consumed. The other metabolite (16%) was due to oxidation on the phenyl group attached to the piperidine. The formation of 3-hydroxytraxoprodil followed Michaelis-Menten kinetics. K_m and V_{max} values for the formation of 3-hydroxytraxoprodil were 1.7 $\pm$ 0.82 μM and 0.66 $\pm$ 0.05 nmol/min/nmol P450, respectively, by nonlinear curve fitting to the Michaelis-Menten equation. The intrinsic clearance (V_{max}/K_m) for the formation of the major oxidative metabolite in human liver microsomal incubations was 0.38 ml/min/nmol P450.

To identify the P450 involved in the formation of 3-hydroxytraxoprodil, microsomes from six human livers were used to examine the metabolism of traxoprodil. The formation rate of 3-hydroxytraxoprodil exhibited a strong correlation with the activity of CYP2D6 catalyzed bufuralol 1′-hydroxylation (r = 0.96) in six human liver

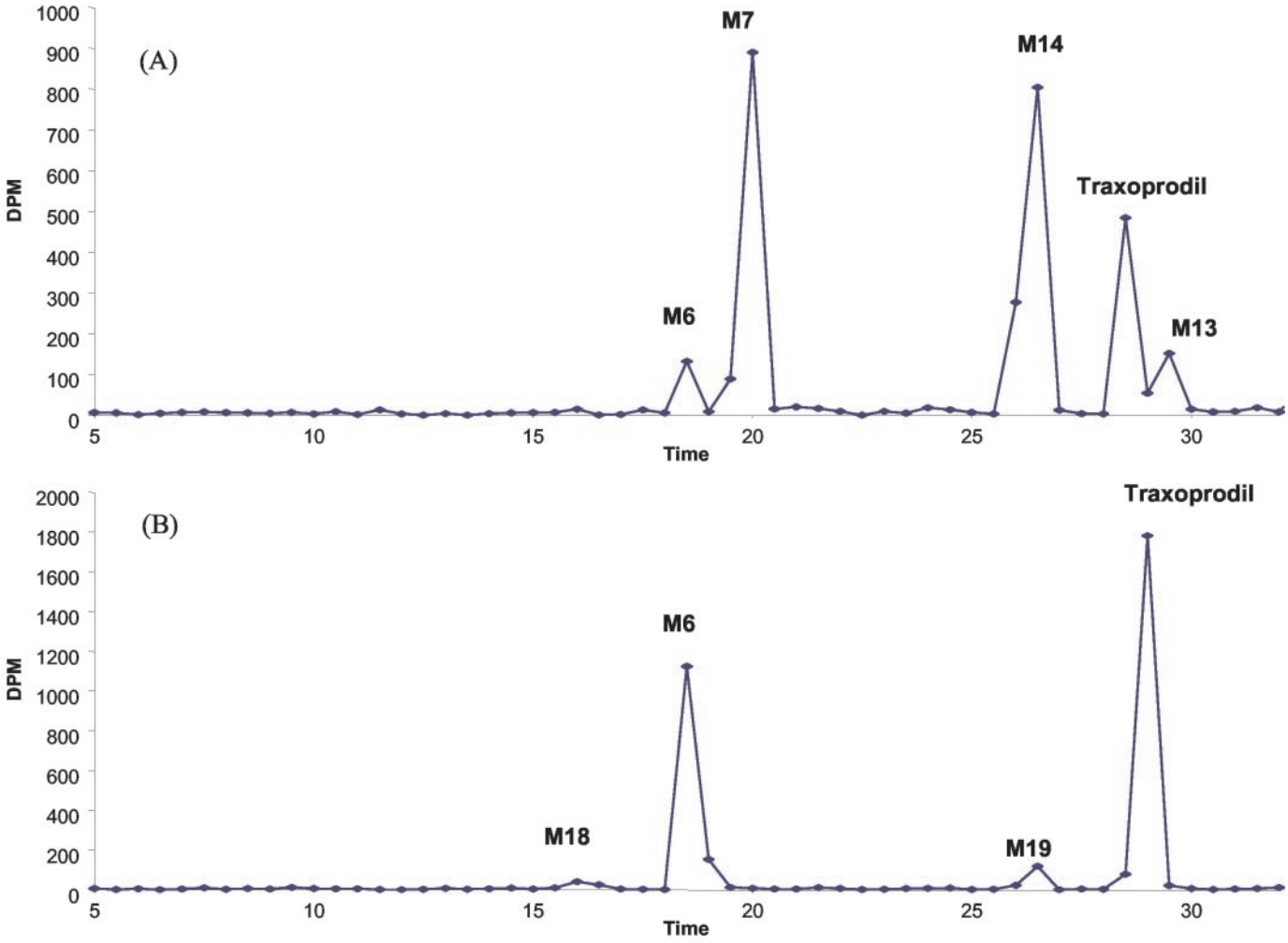

FIG. 6. *HPLC-radiochromatograms of traxoprodil metabolites in human plasma at 6 h of (A) EM and (B) PM after a single i.v. infusion of 50 mg of [^{14}C]traxoprodil.*

TABLE 4

Percentage of circulating metabolites of traxoprodil in humans following 2 h i.v. infusion of a single 50-mg dose of [^{14}C]traxoprodil

	Metabolites						
	M6	M7	M13	M14	M18	M19	Traxoprodil
EM[a]							
2	1.4 ± 0.3	10.5 ± 1.8	5.3 ± 0.9	32.8 ± 5.0	nd	nd	38.3 ± 8.1
6	5.0 ± 1.2	27.9 ± 2.7	5.2 ± 0.6	36.4 ± 3.3	nd	nd	12.9 ± 2.6
24	4.8 ± 2.8	13.8 ± 1.3	4.8 ± 0.9	26.2 ± 11.0	nd	nd	12.5 ± 13.2
PM[b]							
2	6.2, 6.7	nd	nd	nd	1.1, 0.8	4.7, 5.2	79.1, 77.6
6	34.7, 34.7	nd	nd	nd	1.9, 2.1	4.2, 4.0	55.4, 50.7
24	38.8, 35.6	nd	nd	nd	4.4, 2.6	4.0, 4.4	43.7, 46.2

nd, not detected.
[a] EM (N = 4, mean ± S.D.).
[b] PM (N = 2, individual values).

microsomes suggesting that CYP2D6 may be involved in the metabolism of traxoprodil.

In parallel, incubations were also conducted in the presence of a specific CYP2D6 inhibitor, quinidine (0.1, 1, 10, and 100 μM). The addition of increasing concentrations of quinidine into microsomal incubations inhibited traxoprodil metabolism in a concentration-dependent pattern. The formation of hydroxy metabolite was inhibited by 44, 70, 80, and 100% in the presence of 0.1, 1, 10, and 100 μM of quinidine, respectively.

Traxoprodil was not metabolized by microsomes from the control cell line (the cell line that was not transfected with CYP2D6 cDNA) in the presence of NADPH, or the CYP2D6 cell line in the absence of NADPH. Whereas, in the presence of NADPH, 0.2 mg/ml of CYP2D6 cell line microsomal protein metabolized 12% traxoprodil.

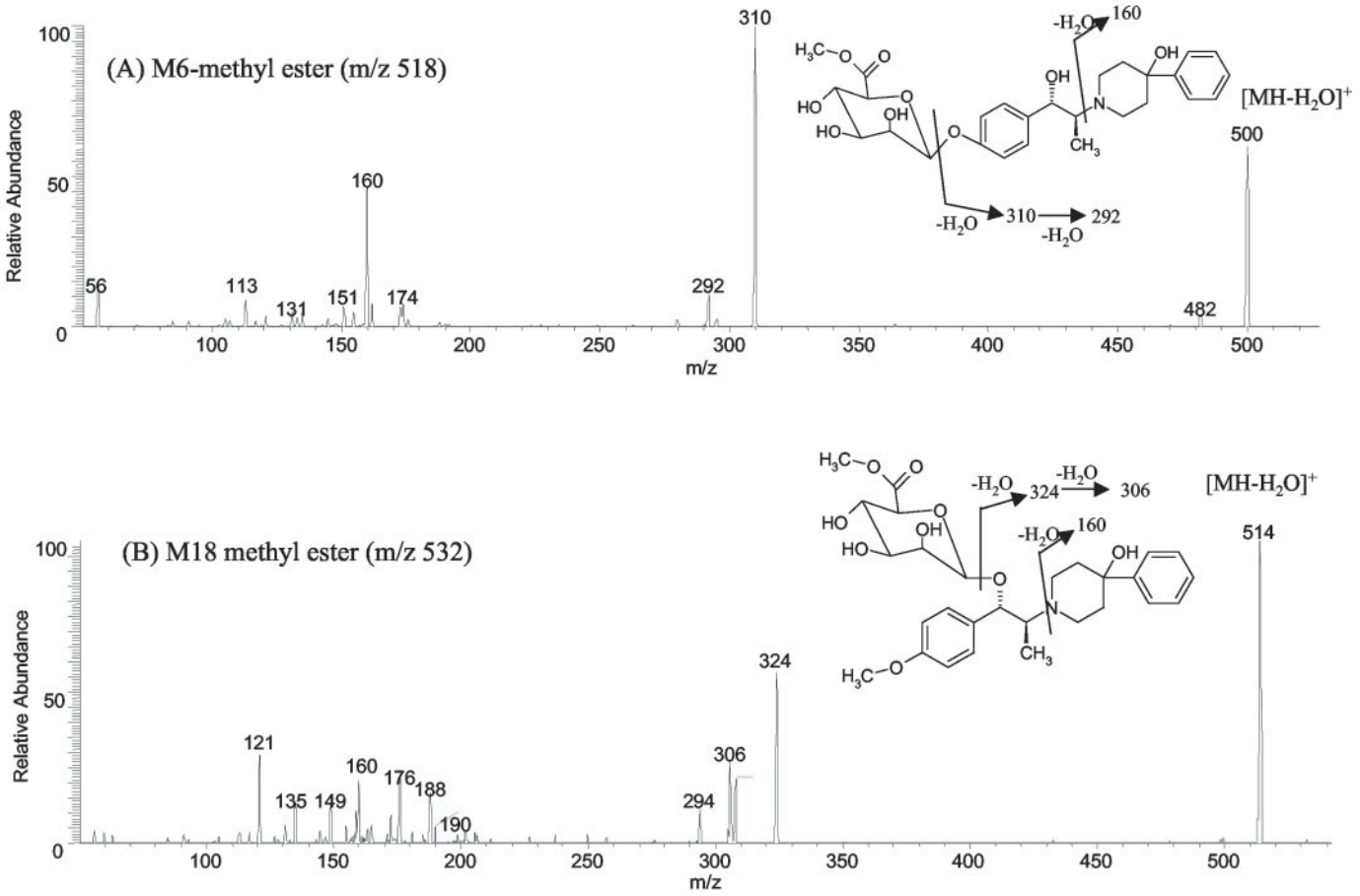

FIG. 7. *CAD product ion mass spectra of metabolites M6 and M18 after treatment with diazomethane (A) m/z 518 (B) m/z 532.*

At higher protein concentration (2 mg/ml), 7.5 μM of traxoprodil was nearly completely metabolized in 40 min.

Discussion

In the present study, the pharmacokinetics, metabolism, and excretion of traxoprodil were investigated in six healthy male volunteers, four subjects phenotyped as CYP2D6 EMs and two subjects as PMs, after a 2 h i.v. infusion of a 50-mg dose of [^{14}C]traxoprodil. The disposition of traxoprodil displayed distinct phenotype related differences in EMs and PMs. The steady-state volume of distribution of traxoprodil was large for both EMs and PMs, suggesting extensive distribution into extravascular tissues. The total CL_p of traxoprodil in EMs was 9-fold greater than in PMs, although the renal clearance of unchanged drug was similar in both the phenotypes. In contrast, $T_{1/2}$ was approximately 10-fold longer in PMs than EMs. These pharmacokinetic parameters were similar to those previously reported for traxoprodil from clinical studies (Merchant et al., 1999). The higher CL_p and shorter half-life for the unchanged drug in EMs than in PMs indicated that the elimination of drug in humans is mediated mainly by CYP2D6. These results were consistent with the recent clinical study in which it was shown that the coadministration of traxoprodil with paroxetine, a specific CYP2D6 inhibitor, significantly altered the disposition of traxoprodil in EMs while it remained unchanged in PMs (Shah et al., 2000).

Plasma levels of the total radioactivity for both EMs and PMs were higher than those for the unchanged traxoprodil, but the difference was more pronounced in EMs than in the PMs. In PMs, mean C_{max}, $AUC_{(0\text{-}Tlast)}$, and $T_{1/2}$ values for total radioactivity were 2- to 3-fold greater than for traxoprodil. While in EMs, mean C_{max} for total radioactivity was 5-fold greater, mean $T_{1/2}$ was 50-fold longer, and mean $AUC_{(0\text{-}Tlast)}$ was 80-fold greater than for traxoprodil itself. These data corroborate the finding in present study that the majority of the circulating radioactivity for EMs is caused by the presence of metabolites with long plasma $T_{1/2}$. The recovery of total radioactivity in excreta was lower in EMs compared with PMs. Approximately 89% of the administered dose was recovered in PMs, similar to that previously obtained in rat and dog (Prakash et al., 1997a). However, only 61% of the administered dose was recovered in EM subjects. Unlike rats and dogs, the majority of the administered radioactive dose was excreted in the urine rather than feces (52% in EMs and 86% in PMs), suggesting that urinary excretion was the primary route of elimination of traxoprodil radioactivity in both EMs and PMs.

Traxoprodil was metabolized in both EMs and PMs and approximately 7.1 and 50.4% of the administered dose was excreted as unchanged drug in the excreta in EMs and PMs, respectively. In addition to traxoprodil, a total of six metabolites were identified by electrospray LC/MS/MS (Fig. 1). There were major phenotype-related qualitative and quantitative differences in the metabolism of traxoprodil in humans. Hydroxylation at the 3-position of the hydroxyphenyl ring followed by conjugation of the resulting catechol was identified as the main metabolic pathway in the EMs. In contrast, the metabolites in PMs were due to direct conjugation with endogenous acids (glucuronic acid or sulfuric acid). The site of glucuronidation was established by enzymatic hydrolysis and chemical derivatization with diazomethane.

The hydroxylation at the hydroxylphenyl ring formed a catechol,

which then underwent *O*-methylation possibly by catechol-*O*-methyltransferase, an enzyme present in liver, red blood cells, and other extrahepatic tissue (Lipsett et al., 1983; Emons et al., 1987). Catechol-*O*-methyltransferase could generate two isomeric monomethyl ethers from the catechol intermediate (i.e., 3-methoxy-traxoprodil and 3-hydroxy-traxoprodil-4-*O*-methyl ether). Therefore, these two regioisomers were synthesized and separated on HPLC system (data not shown). In this study, however, only one regioisomer, 3-methoxy-traxoprodil (M13) was identified by comparison of its chromatographic properties with synthetic standard. Morgan et al. (1969) earlier reported the metabolism of isoproterenol, one of a phenylethylamine, which is resembled in the structure to 3-hydroxytraxoprodil. After i.v. administration of isoproterenol to man, free 3-*O*-methylisoproterenol and its sulfate conjugate were identified as the major metabolites. In case of 2-hydroxyestrogen, the formation of both the regioisomeric methyl ethers (2-OMe-E_2 and 2-OH-E_2-3ME) have been reported (Ball and Knuppen, 1980). However, large differences in the ratios of 2-MeO-E_2: 2-OH-E_2-3ME have been reported when they were assayed in vitro (1:1), in broken cell preparations or intact cells (30:1). 3-Methyoxy-traxoprodil metabolite M13 was followed by conjugation with glucuronic acid or sulfuric acid to form metabolites M7 and M14, respectively. 3-Methoxy-traxoprodil (M13, 2.8%) and its glucuronide (M7, 8.8%) and sulfate (M14, 38.5%) conjugates accounted for ~83% of the excreted radioactivity dose in EMs.

In PMs, glucuronide (M6, 24.6% and M18, 1.4%) and sulfate (M19, 11.7%) conjugates of traxoprodil accounted for ~42% of the excreted radioactivity. The site of conjugation of glucuronides, M6 and M18, was established from the differences in the CAD product ion spectra of their methylated products. After treatment of M6 with diazomethane, Q1 scan of the methylated product showed an intense protonated molecular ion at *m*/*z* 518, 14 Da higher than M6, suggesting that the phenolic group was substituted with glucuronide. On the other hand, the full scan MS of the methylated product of M18 showed an intense protonated molecular ion at *m*/*z* 532, 28 amu higher than M18, indicating the methylation of both phenolic and carboxylic acid groups. Therefore, M18 was characterized as a benzylic glucuronide.

The plasma metabolic profiles in EMs and PMs also showed significant qualitative differences. The amount of circulating unchanged drug was ~6 times greater in the PMs than in the EMs due to the slower rate of metabolism of traxoprodil in PMs. The circulating metabolites were similar to those found in urine. The four metabolites detected in EMs corresponded to unchanged drug, its glucuronide (M6), methylated catechol (M13), its glucuronide (M7), and sulfate (M14) conjugates. The circulating metabolites in PMs were traxoprodil and its glucuronide conjugates (M6 and M18) and sulfate conjugate (M19). Approximately, 96, 95, and 88% of the radioactivity was recovered from the plasma of PMs at 2, 6, and 24 h after extraction. In contrast, the recovery of the radioactivity from the plasma of EMs was 87, 61, and 25% at 2, 6, and 24 h, respectively. These data suggest that oxidative metabolism might have led to covalent binding to plasma proteins in EMs, and this may, in part, be responsible for the low recovery of the administered dose in EMs. Although traxoprodil is extensively hydroxylated in EMs, but the nonconjugated catechol metabolite was not detected either in systemic circulation or in excreta. It is probably due to either rapid conjugative metabolism (*O*-methylation and subsequent glucuronidation or sulfation) followed by urinary excretion or further oxidation to highly reactive *o*-quinone by monooxygenase or peroxidase enzymes, metal ions or molecular oxygen (Monks et al., 1992). Once formed, the *o*-quinone can covalently bind to macromolecules (Bolton et al., 2000). Polyaromatic hydrocarbons (Penning et al., 1999), tamoxifen (Dehl and Kupfer, 1999), and catechol estrogens (Nutter et al., 1991) are some of the classical examples, which are metabolically activated by oxidation to the reactive Michael acceptor *o*-quinone, and form stable DNA adducts. Covalent binding of traxoprodil metabolites to proteins and an elucidation of its mechanism(s) are subjects of further investigation.

Results obtained after incubation of traxoprodil with human liver microsomes demonstrated the formation of one major metabolite (3-hydroxytraxoprodil). Further in vitro studies using CYP2D6 selective inhibitor, correlation of metabolite formation with bufuralol-1′-hydroxylase activity, and recombinant enzyme have also suggested that the metabolism of traxoprodil is mainly metabolized by CYP2D6, a major drug-metabolizing enzyme that exhibits genetic polymorphism (Meyer and Zanger, 1997). These results coincide exactly with in vivo data in the sense that the oxidative metabolites were detected only in the EMs. Approximately 7 to 10% of the white population shows an inherited deficiency in this enzyme due to the presence of one or several mutant alleles at the CYP2D6 gene locus (Hanioka et al., 1990). These subjects are characterized by the PM phenotype. Compared with normal or EMs, PM subjects demonstrate markedly greater AUC values for parent drugs that are metabolized by CYP2D6 and therefore require lower doses to achieve therapeutic effects (Kivisto and Kroemer, 1997). In this study, we observed higher plasma concentrations and AUC values for unchanged traxoprodil in the PMs as compared with the EMs, thus providing additional evidence that traxoprodil is a substrate for CYP2D6.

In conclusion, traxoprodil is metabolized in both EMs and PMs after i.v. infusion, and the radioactive dose is excreted mainly in urine. The compound displayed notable phenotype-related differences in pharmacokinetic and metabolic behavior in EMs and PMs and eliminated by Phase II metabolism and renal clearance of parent in PMs and by oxidation followed by conjugation in EMs. In addition, there were significant differences in the plasma concentrations of the unchanged drug in EMs and PMs. Therefore, it can be concluded that the metabolism of traxoprodil cosegregates with the *O*-demethylation of dextromethorphan, a probe substrate for monitoring the CYP2D6 activity.

Acknowledgments. We thank Dr. Keith McCarthy and Dr. Kathleen Zandi and Sandra Miller for providing radiolabeled traxoprodil; Dr. Bertrand Chenard and Todd Butler for the synthesis of synthetic standards; Dr. Aziz Laurent for conducting the dosing and sample collections; Robert Walski, Beth Obach, Carman Sanchez, and Terry Morse for technical assistance and Dr. Cheryl Bye, Dr. Joe Mongillo, Dr. Marie Reynolds, Randy Bouley, Dr. Peter Thompson, and Nancy Chin for their efforts in the release testing of traxoprodil. We also thank Dr. Larry Tremaine for critical evaluation of the manuscript.

References

Balant LP and Gex-Fabry M (1994) Dealing with variability during drug development. *J Pharm Pharmacol* **46 (Suppl 1):**439–444.

Ball P and Knuppen R (1980) Catecholestrogens (2- and 4-hydroxyestrogens): chemistry, biogenesis, metabolism, occurrence and physiological significance. *Acta Endocrinol* **232 (Suppl):**1–127.

Bolton JL, Trush MA, Penning TM, Dryhurst G, and Monks TJ (2000) Role of quinones in toxicology. *Chem Res Toxicol* **13:**135–160.

Boyce S, Wyatt A, Webb JK, O'Donnell R, Mason G, Rigby M, Sirinathsinghji D, Hill RG, and Rupniak NM (1999) Selective NMDA NR2B antagonists induce antinociception without motor dysfunction: correlation with restricted localization of NR2B subunit in dorsal horn. *Neuropharmacology* **38:**611–623.

Bullock MR, Merchant RE, Carmack CA, Doppenberg E, Shah AK, Wilner KD, Ko G, and Williams SA (1999) An open-label study of CP-101, 606 in subjects with a severe traumatic head injury or spontaneous intracerebral hemorrhage. *Ann NY Acad Sci* **890:**51–58.

Chenard BL, Bordner J, Butler TW, Chambers LK, Collins MA, De Costa DL, Ducat MF, Dumont ML, Fox CB, Mena EE, et al. (1995) (1*S*,2*S*)-1-(4-hydroxy-phenyl)-2-(4-hydroxy-4-phenyl-piperidino)-1-propanol: a potent new neuroprotectant which blocks of *N*-methyl-D-aspartate responses. *J Med Chem* **38:**3138–3145.

Dehl SS and Kupfer D (1999) Cytochrome P-450 3A and 2D6 catalyze ortho hydroxylation of

4-hydroxytamoxifen and 3-hydroxytamoxifen (droloxifene) yielding tamoxifen catechol: involvement of catechols in covalent binding to hepatic proteins. *Drug Metab Dispos* **27:**681–685.

Di X, Bullock R, Watson J, Fatouros P, Chenard B, White W, and Corwin F (1997) Effect of CP-101, 606, a novel NR2B subunit antagonist of *N*-methyl-D-aspartate receptor, on the volume of ischemic brain damage and cytotoxic brain edema after cerebral artery occlusion in the feline brain. *Stroke* **28:**2244–2251.

Emons G, Marriam G, Pfeiffer D, Loriaux D, Ball P, and Knuppen R (1987) Metabolism of exogenous 4- and 2-hydroxyestradiol in the human male. *J Steroid Biochem* **28:**499–504.

Hanioka N, Kimura S, Meyer UA, and Gonzalez FJ (1990) The human CYP2D6 locus associates with a common genetic defect in drug oxidation: a G1934 to a base change in intron 3 of a mutant CYP2D6 allele results in an aberrant 3′ splice recognition site. *Am J Hum Genet* **47:**994–1001.

Kivisto KT and Kroemer HK (1997) Use of probe drugs as predictors of drug metabolism in humans. *J Clin Pharmacol* **37:**40S–48S.

Kronbach T, Mathys D, Gut J, Catin T, and Meyer UA (1987) High-performance liquid chromatographic assays for bufuralol 1′-hydroxylase, debrisoquine 4-hydroxylase and dextromethorphan *O*-demethylase in microsomes and purified cytochrome P-450 isozymes of human liver. *Anal Biochem* **162:**24–32.

Lipsett M, Merriam G, Kono S, Brandon D, Pfeiffer D, and Loriaux D (1983) Metabolic clearance of catechol estrogens, in *Catechol Estrogens* (Merriam G and Lipsett M eds) pp 105–114, Raven Press, New York.

McCarthy KE, Miller SA, Chenard BL, Butler TW, Dumont ML, and Stemple JZ (1997) Synthesis of high specific activity tritium and optically pure [^{14}C]-CP-101, 606. Enantioselective crystalization of a radiochemically racemic mixture. *J Label Compd Radiopharm* **39:**973–985.

Meier UT, Kronbach T, and Meyer UA (1985) Assay of mephenytoin metabolism in human liver microsomes by high-performance liquid chromatography. *Anal Biochem* **151:**286–291.

Menniti FS, Chenard BL, Collins MA, Ducat MF, Shalaby IA, and White WF (1997) CP-101, 606: a potent neuroprotectant selective for forebrain neurons. *Eur J Pharmacol* **331:**117–126.

Menniti FS, Pagnozzi MJ, Butler P, Chenard BL, Jaw-Tsai S, and White WF (2000) CP-101, 606, an NR2B subunit selective NMDA receptor antagonist inhibits NMDA and injury induced c-fos expression and cortical spreading depression in rodents. *Neuropharmacology* **39:**1147–1155.

Menniti FS, Shah AK, Williams SA, Wilner KD, White WF, and Chenard BL (1998) CP-101, 606: an NR2B-selective NMDA receptor antagonist. *CNS Drug Rev* **4:**307–322.

Merchant RE, Bullock MR, Carmack CA, Shah AK, Wilner KD, Ko G, and Williams SA (1999) A double-blind, placebo-controlled study of the safety, tolerability and pharmacokinetics of CP-101, 606 in patients with a mild or moderate traumatic brain injury. *Ann NY Acad Sci* **890:**42–50.

Meyer UA and Zanger UM (1997) Molecular mechanism of genetic polymorphisms of drug metabolism. *Annu Rev Pharmacol Toxicol* **17:**269–296.

Miners JO, Smith KJ, Robson RA, McManus ME, Veronese ME, and Birkett DJ (1988) Tolbutamide hydroxylation by human liver microsomes. Kinetic characterization and relationship to other cytochrome P-450 dependent xenobiotic oxidations. *Biochem Pharmacol* **37:**1137–1144.

Monks TJ, Hanzlik RP, Cohen GM, Ross D, and Graham DG (1992) Contemporary issues in toxicology: quinone chemistry and toxicity. *Toxicol Appl Pharmacol* **112:**2–16.

Morgan D, Sandler M, Davies S, Conolly M, Paterson J, and Dolley CT (1969) Metabolic fate of DL-isoprenaline 7–3H in man and dog. *Biochem J* **114:**8P.

Nutter LM, Ngo EO, and Abul-Hajj YJ (1991) Characterization of DNA damage induced by 3,4-estrone-*o*-quinone in human cells. *J Biol Chem* **266:**16380–16386.

Omura T and Sato R (1964) The carbon monoxide binding pigment of liver microsomes. I. Evidence of its hemoprotein nature. *J Biol Chem* **239:**2370–2378.

Penning TM, Burczynski ME, Hung CF, McCoull KD, Palackal NT, and Tsuruda LS (1999) Dihydrodiiol dehydrogenases and polycyclic aromatic hydrocarbon activation: generation of reactive and redox active o-quinones. *Chem res Toxicol* **12:**1–18.

Prakash C, Cui D, and Johnson K (1997a). Biotransformation of a NMDA receptor antagonist, CP-101, 606, in Long-Evans rats: characterization of glucuronide conjugates by mass spectrometry. *8th North American ISSX Meeting*; 1997 October 26–30; Hilton Head, SC. International Society for the Study of Xenobiotics, Cabin John, MD.

Prakash C, Kamel A, Cui D, Whalen R, Miceli J, and Tweedie D (2000) Identification of the major human liver cytochrome P450 isoform responsible for the formation of the primary metabolites of ziprasidone and prediction of possible drug interactions. *Br J Clin Pharmacol* **49 (Suppl):**35S–42S.

Prakash C, Kamel A, Gummerus J, and Wilner K (1997b) Metabolism and excretion of the antipsychotic drug, ziprasidone, in humans. *Drug Metab Dispos* **25:**863–872.

Prakash C and Soliman V (1997) Metabolism and excretion of a new anxiolytic drug candidate, CP-93, 393, in Long-Evans rat. *Drug Metab Dispos* **25:**1288–1297.

Shah AK, Friedman DL, Morse TM, Laboy-Goral L, Hinkel CA, Silber M, Apseloff G, and Friedman HL (1998) Evaluation of methods for rapid screening of CYP2D6 status using dextromethorphan as a probe in normal healthy subjects. *Pharm Sci* **1:**S-32.

Shah AK, Sanchez CS, Morse TA, and Friedman H (2000) The effect of coadministartion of a CYP2D6 inhibitor on the oral pharmacokinetics (PK) of CP-101, 606 in healthy subjects. 10th North American ISSX Meeting, Indianapolis, IN. International Society for the Study of Xenobiotics, Cabin John, MD.

Sonderfan AJ, Arlotto MP, Dutton DR, McMillen SK, and Parkinson A (1987) Regulation of testosterone hydroxylation by rat liver microsomal cytochrome P-450. *Arch Biochem Biophy* **255:**27–41.

Taniguchi K, Shinjo K, Mizutani M, Shimada K, Ishikawa T, Menniti F, and Nagahisha A (1997) Antinociceptive activity of CP-101, 606, an NMDA receptor NR2B subunit antagonist. *Br J Pharm* **122:**809–812.

Tassaneeyakul W, Birkett DJ, Veronese ME, McManus ME, Tukey RH, Quattrochi LC, Gleboin HV, and Miners JO (1993) Specificity of substrate and inhibitor probes for human cytochromes P450 1A1 and 1A2. *J Pharmacol Exp Ther* **265:**401–407.

Tsuchida E, Rice M, and Bullock R (1997) The neuroprotective effect of the forebrain-selective NMDA antagonist CP-101, 606 upon focal ischemic brain damage caused by acute subdural hematoma in the rat. *J Neurotrauma* **14:**409–417.